Cell Tissue Res (2005) 321: 273–284
DOI 10.1007/s00441-005-1118-4

REGULAR ARTICLE

Sonja Kleinlogel · N. Justin Marshall

Photoreceptor projection and termination pattern in the lamina of gonodactyloid stomatopods (mantis shrimp)

Received: 13 January 2005 / Accepted: 9 March 2005 / Published online: 10 June 2005

Abstract The apposition co mpound eyes of gonodactyloid stomatopods are divided into a ventral and a dorsal hemisphere by six equatorial rows of enlarged ommatidia, the mid-band (MB). Whereas the hemispheres are specialized for spatial vision, the MB consists of four dorsal rows of ommatidia specialized for colour vision and two ventral rows specialized for polarization vision. The eight retinula cell axons (RCAs) from each ommatidium project retinotopically onto one corresponding lamina cartridge, so that the three retinal data streams (spatial, colour and polarization) remain anatomically separated. This study investigates whether the retinal specializations are reflected in differences in the RCA arrangement within the corresponding lamina cartridges. We have found that, in all three eye regions, the seven short visual fibres (svfs) formed by retinula cells 1–7 (R1–R7) terminate at two distinct lamina levels, geometrically separating the terminals of photoreceptors sensitive to either orthogonal e-vector directions or different wavelengths of light. This arrangement is required for the establishment of spectral and polarization opponency mechanisms. The long visual fibres (lvfs) of the eighth retinula cells (R8) pass through the lamina and project retinotopically to the distal medulla externa. Differences between the three eye regions exist in the packing of svf terminals and in the branching patterns of the lvfs within the lamina. We hypothesize that the R8 cells of MB rows 1–4 are incorporated into the colour vision system formed by R1–R7, whereas the R8 cells of MB rows 5 and 6 form a separate neural channel from R1 to R7 for polarization processing.

This research was supported by the Swiss National Science Foundation (PBSKB-104268/1), the Australian Research Council (LP0214956) and the American Air Force (AOARD/AFOSR) (F62562-03-P-0227).

S. Kleinlogel (✉) · N. J. Marshall
Vision, Touch and Hearing Research Centre,
School of Biomedical Sciences, University of Queensland,
Brisbane, 4072, Australia
e-mail: S.Kleinlogel@uq.edu.au
Tel.: +61-7-33653127
Fax: +61-7-33654522

Keywords Visual system · First optic ganglion · Long visual fibres · Short visual fibres · Gonodactyloid stomatopods · Shrimp · *Haptosquilla glyptocercus* · *Gonodactylus chiragra* (Crustacea)

Abbreviations epl_1: Outer lamina stratum · epl_2: inner lamina stratum · lvf: long visual fibre · MB: mid-band · MPA: axial monopolar cell · MPL: lateral monopolar cell · RCA: retinula cell axon · R1–R8: retinula cells 1–8 · svf: short visual fibre

Introduction

Gonodactyloid stomatopod crustaceans inhabit shallow, well-lit, and therefore spectrally rich, tropical and subtropical seas. They are aggressive diurnal predators that also exhibit complex social behaviour. This frequently involves the display of a great diversity of coloured and polarized body markings (Caldwell and Dingle 1975, 1976; Cronin and Marshall 2004). They possess true colour and polarization vision (Marshall et al. 1996; Marshall and Oberwinkler 1999). The apposition compound eyes of gonodactyloids are of an elaborate trinocular design, which appears to be unique in the animal kingdom (Marshall 1988; Marshall et al. 1989, 1991b). They consist of a dorsal and a ventral hemisphere bisected by an equatorial band of six rows of enlarged ommatidia, the mid-band (MB). The hemispheric retinas are typical of other crustacean eyes. They contain two spectral sensitivities and are believed to mediate spatial vision and motion detection (Land et al. 1990; Marshall and Land 1993a,b; Cronin et al. 1994b). The MB, however, is again divided into four dorsal rows that are anatomically and functionally specialized for colour vision (MB rows 1–4) and two ventral rows that are specialized for polarization vision (MB rows 5 and 6; Marshall et al. 1991a,b; Cronin et al. 1994b). Consequently, stomatopod eyes are divided into three functionally distinct retinal areas: the hemispheres for spatial vision, MB rows 1–4 for colour vision and MB rows 5 and 6 for polarization vision.

The fused rhabdoms of gonodactyloid stomatopods are composed of seven long retinula cells (R1–R7) and one short eighth retinula cell (R8), the latter forming the distal part of the ommatidium (Marshall 1988; Marshall et al. 1991b). In the hemispheres and MB rows 5 and 6, the R1–R7 cells are similar to those of other malacostracan crustaceans (Nässel 1975; Strausfeld and Nässel 1981). They possess identical spectral sensitivities (green) and are divided into two cell groups (R1, R4, R5 and R2, R3, R6, R7), which possess orthogonal layers of microvilli (Goldsmith and Fernandez 1968; Waterman 1981; Ball et al. 1986; Marshall et al. 1991b). These two cell groups have been suggested to form two opposing information channels of polarized light (Waterman and Fernandez 1970; Bernard and Wehner 1977; Stowe et al. 1977; Waterman 1981; Sabra and Glantz 1985; Marshall et al. 1991b). In MB rows 5 and 6 of the stomatopod, the layers of microvilli are thin and particularly highly ordered, which suggests that their R1–R7 cells possess high polarization sensitivity (Marshall et al. 1991b). In MB rows 1–4, the two cell groups (R1, R4, R5 and R2, R3, R6, R7) have become modified from the basic crustacean R1–R7 rhabdom to form two separate retinal tiers. These tiers contain different visual pigments and possess different spectral sensitivities (Cronin and Marshall 1989; Cronin et al. 1994a). Each retinula cell has orthogonally arranged microvilli and this greatly reduces its overall sensitivity to polarized light (Marshall et al. 1991b). Therefore, MB rows 1–4 have been hypothesized to represent an area of photoreceptors that mediate colour vision (Marshall 1988; Cronin and Marshall 2004). As in other crustaceans with fused rhabdoms, the eight RCAs emanating from each ommatidium project retinotopically to the first optic neuropile, the lamina, innervating one underlying lamina unit (cartridge) and thus preserving spatial information (Kleinlogel et al. 2003). Here, the seven short visual fibres (svfs) originating from R1–R7 form terminals and connect with second-order interneurons, the monopolar ganglion cells, which convey visual information directly to the second optic neuropile, the medulla externa. Information leaving the stomatopod retina is divided into three parallel data streams (presumed spatial, spectral and polarization), which project to discrete zones of the underlying neuropiles (Kleinlogel et al. 2003). The lamina and the medulla externa possess elevated equatorial neuropile areas (accessory lobes), which receive inputs exclusively from the retinal MB (Kleinlogel et al. 2003). Colour and polarization information are represented in parallel zones of the accessory lobes (Kleinlogel et al. 2003).

Although much is known about the intriguing retinal capabilities of gonodactyloid stomatopods (Cronin and Marshall 1989; Marshall et al. 1989, 1991a,b; Cronin et al. 1994a; Marshall and Oberwinkler 1999), the way in which visual information is processed is still poorly understood. Lamina cartridges of the three functionally different eye regions can be anatomically distinguished by using low-magnification light microscopy: lamina cartridges of MB rows 1–4 are rectangular in shape, lamina cartridges of MB rows 5 and 6 are oval and hemispheric cartridges are hexagonal (Kleinlogel et al. 2003). To determine whether this is attributable to differences in the RCA projection and termination pattern within the lamina, we have used a combination of light microscopy of intracellularly stained photoreceptors (serial sections) and electron microscopy.

Materials and methods

Animals

The results were obtained from male and female stomatopods of the superfamily Gonodactyloidea. Species used were mainly *Haptosquilla glyptocercus* and *Gonodactylus chiragra* but with some comparison with *Chorisquilla trigibbosa*, *Pseudosquilla ciliata*, *Gonodactylus smithii*, *Haptosquilla trispinosa* and *Gonodactylus platysoma*. Adult animals were collected on Heron and Lizard Islands (GBR MPA permit no. G00/023). The animals were shipped to the University of Queensland and kept in marine aquaria approved by the Australian Quarantine Inspection Service and Environment Australia Wildlife Protection under a 12 h dark/12 h light cycle. Overhead lighting was from UV-enhanced fluorescent light-sources ("TL"D natural light and Blacklight) directly above the tanks. Animals were killed by decapitation. All procedures were approved by the Animal Ethics Committee (permit no. 463/04) of the University of Queensland.

Terminology

The eyestalks of malacostracan crustaceans contain four successive columnar optic neuropiles underlying the retina; these neuropiles are classically called the lamina ganglionaris, medulla externa, medulla interna and medulla terminalis (Hanström 1928). We adhere to this terminology in stomatopods with one exception, viz. the lamina ganglionaris. Since there is a clear analogy between the crustacean lamina ganglionaris and the insect lamina, the insect terminology is applied here (Strausfeld and Nässel 1981; Nilsson and Osorio 1997; Kleinlogel et al. 2003). We refer to Marshall et al. (1991a) for the numbering of retinula cells (R1–R8) in the retina. The RCAs originating in the R1–R7 cells are specified as svfs and the RCA originating in the distal R8 cell is referred to as the lvf. The terminology used for tissue orientation is explained in Fig. 1.

Tracing of photoreceptor and monopolar ganglion cell axons

Three complete sets (two from *H. glyptocercus* and one from *G. chiragra*) of RCA fascicles from five to ten neighbouring ommatidia of each MB row and one row of each hemisphere were traced from the retina to the proximal margin of the lamina under the light and electron microscope (for a detailed description of the method, see Kleinlogel et al. 2003). Additional less extensive sets were obtained from other gonodactyloid species (*G. chiragra*, *H. glyptocercus*,

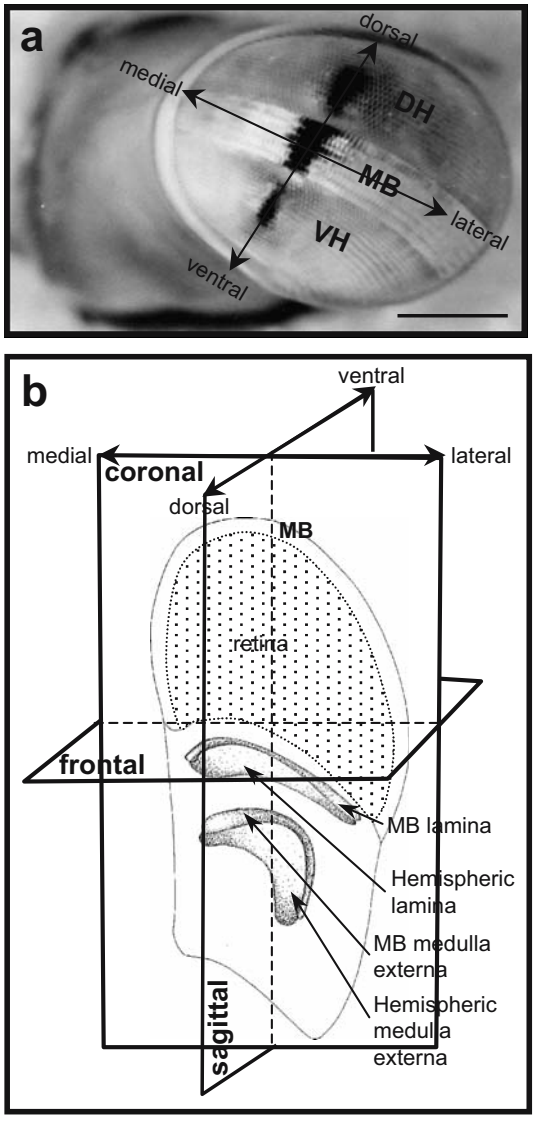

Fig. 1 **a**, **b** Terminology of eye orientation, here shown for a right eye. Unless otherwise stated, the descriptions in the text are always made for a right eye. In the following, all frontal sections are viewed as if looking into the eye. **a** The eye is divided into a dorsal (*DH*) and a ventral (*VH*) hemisphere by a six-rowed band of enlarged ommatidia, the mid-band (*MB*). **b** Diagram of a dorsal view of the eye showing the position of the lamina and the medulla externa within the eyestalk and the three planes of sectioning. The lamina and the medulla externa are divided into a main body subserved by fibres from the hemispheres and an elevated accessory lobe subserved by fibres from the *MB*. *Bar* 1 μm

H. trispinosa, *C. trigibbosa*, *P. ciliata* and *G. smithii*). Whole eyes were fixed overnight in 2.5% glutaraldehyde in 0.1 M PIPES buffer (sesquisodium salt, ICN Biomedicals, Ohio, USA) containing 15% sucrose and 10 mM EGTA, postfixed for 2 h on ice (with the eyestalk removed) in a mixture of 1% osmium tetroxide and 1.5% potassium ferricyanide, dehydrated in ethanol and embedded in hard Spurr's. The retina-to-lamina projection pathways of the eight RCAs emanating from each ommatidium were reconstructed from serial semi-thin frontal sections for light microscopy. The axons of the five monopolar ganglion cells were classified by determining their cell body position within pseudocartridges. In order to trace the position of the axon profiles of photoreceptor and monopolar ganglion cells throughout the lamina, thin sections for electron microscopy were cut alternating with semi-thin sections for light microscopy. Thin sections with a silver or grey interference colour were obtained by using diamond knives. They were collected on uncoated copper grids and stained with 5% uranyl acetate followed by lead citrate (Reynolds 1963) for study in a JEOL 1010 transmission electron microscope. Axon profiles in transmission electron micrographs were numbered according to the corresponding semi-thin sections. Photographs were digitized on a Leafscan 45 (Leaf systems, Mass., USA) and, in some instances, modified in brightness and contrast by using Adobe Photoshop 6.0 (Adobe Systems, Mountain View, Calif., USA).

Lucifer yellow injections

A total of 96 svfs (69 of *G. chiragra*, 27 of *H. glyptocercus*) and 31 lvfs (21 of *G. chiragra*, 10 of *H. glyptocercus*) were injected with Lucifer yellow in order to confirm the photoreceptor terminal numbering in the lamina previously determined by serial light microscopy (Kleinlogel et al. 2003) and to visualize the photoreceptor morphology. Each photoreceptor type was injected and traced at least once (Table 1). The entire procedure was performed under a photographic safelight to avoid light adaptation of the photoreceptors. Whole eyes were waxed onto a rotatable plastic rod and the MB was oriented horizontally. The rod was then immersed in saline and a small hole was cut in either the dorsal or the ventral hemisphere. Thick-walled borosilicate microelectrodes (WPI, OD/ID 1.2/0.68 mm) were pulled on a Sutter P-97 puller and their tips were filled with 8% Lucifer yellow CH (Sigma) in 0.1 M TRIS buffer (70–180 MΩ). The preparation was then placed into a cardan arm arrangement (Warrant and McIntyre 1990) and an Ag/AgCl pellet immersed in saline was used as an reference electrode. The recording electrode was lowered vertically through the hole and into the retina. Penetration of a photoreceptor was identified by a sudden voltage drop and an unambiguous response to a flash of white light. A

Table 1 Overview of the number of Lucifer yellow injected retinula cells in *Gonodactylus chiragra* (*Gc*) and *Haptosquilla glyptocercus* (*Hg*). For simplification, retinula cells 1–7 (*R1–R7*) are listed as cell groups sensitive to identical wavelengths or e-vector directions of light (*DH* dorsal hemisphere, *VH* ventral hemisphere, *MB1–6* mid-band rows 1–6).

Retinula cells	Species	DH	MB1	MB2	MB3	MB4	MB5	MB6	VH
R1, R4, R5	*Gc*	8	6	3	5	3	2	3	6
	Hg	1	3	0	2	0	2	1	3
R2, R3, R6, R7	*Gc*	6	4	3	3	4	3	5	5
	Hg	3	2	1	2	3	1	1	2
R8	*Gc*	5	4	1	3	2	2	1	3
	Hg	2	2	1	2	0	1	2	0

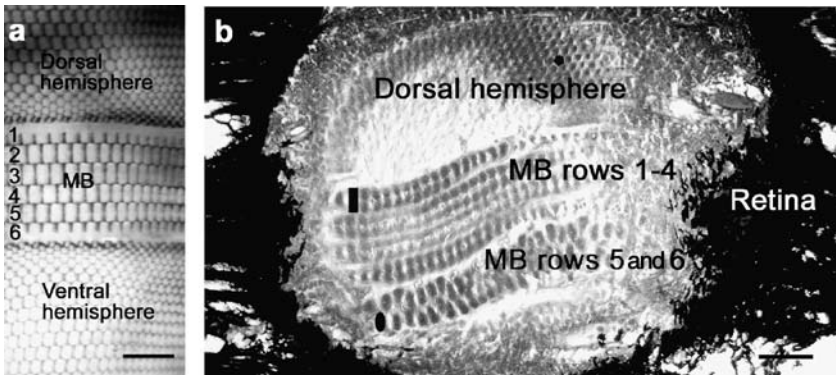

Fig. 2 **a**, **b** The hemispheres form small hexagonal facet lenses, whereas the mid-band (*MB*) forms enlarged rectangular facets (**a**) and this mosaic is reflected by the neural organization of the lamina (**b**). In frontal sections through the outer lamina stratum (epl_1) (*light tissue*), the lamina cartridges of the three eye regions are differently shaped. Because of the curvature of the eye, parts of the retina are also seen at the edges of the section (*dark tissue*). Lamina cartridges of the hemispheres are hexagonal in shape, cartridges of *MB* rows 1–4 are rectangular in shape and cartridges of *MB* rows 5 and 6 are oval. *Bars* 50 μm

hyperpolarizing DC current of 0.15–0.7 nA in a 1 Hz duty cycle regime was applied for 15–20 min in order to stain the impaled cell. After injection with Lucifer yellow, the eye was fixed in 4% paraformaldehyde, 0.25% glutaraldehyde and 30% sucrose in 0.1 M phosphate buffer for 2–3 days at 4°C. The tissue was dehydrated with ethanol and embedded in frontal, coronal and sagittal orientations in 2-hydroxyethylmethacrylate (Technovit T7100, Heraeus, Germany). Serial plastic sections (7 μm thick) were cut on a historange microtome (LKB), collected on SuperFrost Plus slides (Menzel) and coverslipped with fluorescent mounting medium (DAKO). Sections were viewed and photographed under a Zeiss Axioskop microscope equipped with a digital SPOT camera by using fluorescence microscopy and ALPHA Vivid standard Lucifer yellow XF14 filters (OMEGA OPTICAL). Samples of particular interest were

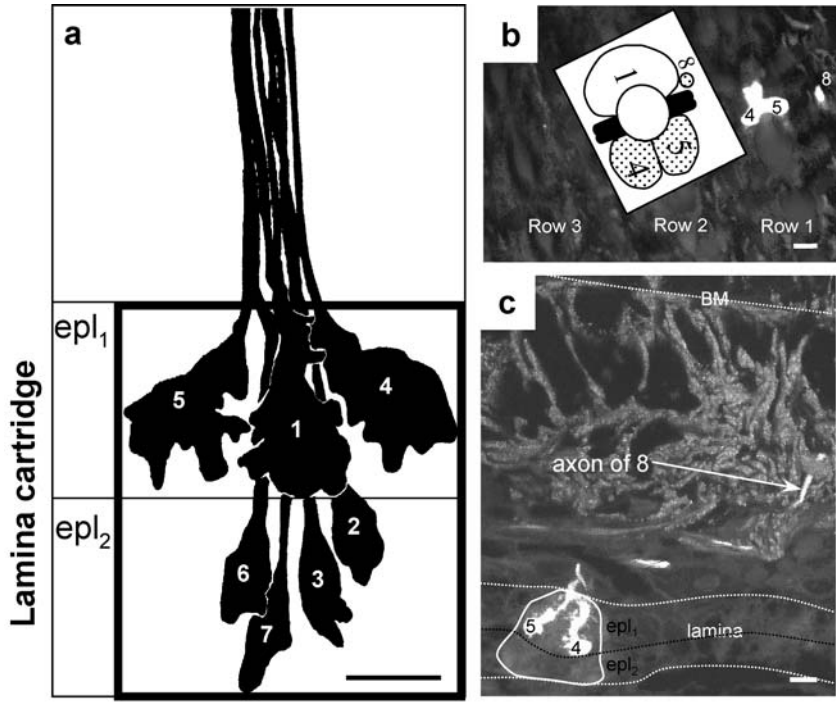

Fig. 3 **a**–**c** Termination pattern of the seven short visual fibres (*svfs*) of mid-band row 1 at two lamina strata. **a** Schematic diagram of the arrangement and morphology of the svf terminals (*1–7*) in the lamina. For simplification, the axons of the long visual fibre and of the monopolar ganglion cells are not depicted. Svf1, svf4 and svf5 end in the outer lamina stratum (epl_1) in enlarged bag-like terminals of about 5 μm in diameter with an extensive array of fine branches. The terminals of svf2, svf3, svf6 and svf7 terminate in the inner lamina stratum (epl_2). They are smaller and form fewer spines. The terminal of svf7 extends the furthest proximally. **b** Lucifer-yellow-injected retinula cells 4, 5 and 8 viewed in a frontal 7-μm-thick plastic section. The retinula cell arrangement at the level of the section is shown in the schematic *inset*. **c** Sagittal 7-μm-thick plastic section from the same series as in **b** showing the dilated and spiny terminals of svf4 and svf5 in epl_1. The axon of the long visual fibre (*axon of 8*) is seen projecting to the lamina (*BM* basement membrane). *Bars* 5 μm

viewed by using a Nikon E600 confocal microscope with 40×/1.3, 60×/1.4 and 100×/1.4 oil immersion lenses. Profiles of stained cells were scanned with a Bio-Rad radiance 2000 confocal laser scanning microscope and Bio-Rad Lasersharp 2000 software. Confocal projections were composed of a series of 20 images collected to a depth of 7 μm at 0.35-μm intervals. Collected images were then processed and enhanced in contrast by using Adobe Photoshop 6.0. Morphologies of filled neurons were reconstructed from serial confocal projections, which were overlaid as aligned stacks and flattened to one plane with the use of Photoshop 6.0 (Adobe Systems).

Results

The lamina of gonodactyloid stomatopods is a curved neuropile, measuring about 20 μm in thickness (Fig. 1b). Here, the RCA bundles are regularly arranged and distinctly delineated by a network of tangentially oriented glial cell fibres (Fig. 2). The arrangement of RCAs and interneurons within each cartridge is precise and reiterated. The synaptic region of the lamina (the external plexiform layer) can be divided into two layers, epl_1 and epl_2 (Fig. 3a). These layers, both about 10 μm thick, are the result of the different levels of svf endings. Of the eight RCAs originating in each retinal ommatidium, seven terminate in the lamina. The svfs formed by R1, R4 and R5 (svf1, svf4, svf5) terminate in epl_1 and the svfs formed by R2, R3, R6 and R7 (svf2, svf3, svf6, svf7) in epl_2. The lvfs pass through the lamina cartridge and the first optic chiasm to reach the distal medulla externa (see Fig. 6a). This general RCA arrangement is identical in the laminae of all three eye regions (hemispheres, MB rows 1–4 and MB rows 5 and 6). Each lamina cartridge contains five monopolar ganglion cell axons (Fig. 4a). Three originate in the outer monopolar cell layer and project together with the lvf axially through the lamina cartridge (Kleinlogel et al. 2003; Figs. 4a, b, 5). They are therefore referred to as axial monopolar ganglion cells (MPAs). The two remaining monopolar ganglion cell axons originate in the inner monopolar cell layer and line the lamina cartridges medially and laterally together with glial cell processes and are referred to as lateral monopolar ganglion cells (MPLs; Kleinlogel et al. 2003; Figs. 4a, b, 5). Below the lamina, the axon bundles emanating from single lamina cartridges contain the five monopolar ganglion cell axons and the axially situated axon of the lvf (Fig. 4c).

Two lamina strata

The seven svfs end in enlarged bag-like terminals of 5 μm in diameter; three (svf1, svf4 and svf5) in the epl_1 and four (svf2, svf3, svf6 and svf7) in the epl_2. This anatomical division separates the two cell groups of different polarization (hemispheres and MB rows 5 and 6) or spectral (MB rows 1–4) sensitivities within each ommatidium (Figs. 3, 4a, b, 5). Photoreceptor terminals derived from MB row 2 ommatidia show identical layering within the lamina, even though the groups of retinula cells forming the two retinal tiers in this row are inverted (Marshall et al. 1991b; Kleinlogel et al. 2003). The terminals of svf1, svf4 and svf5, which terminate in the epl_1, form dilated endings with a wide array of fine branches, sometimes extending over half of the lamina cartridge (Fig. 3). Hemispheric terminals in the epl_1 have a diameter of 3–4 μm, those of MB rows 5 and 6 are 4–5 μm in diameter and terminals of MB rows 1–4 are 5–6 μm in diameter (Figs. 4a, 5). In contrast, the terminals of svf2, svf3, svf6 and svf7, which terminate in the epl_2, are smaller and more tightly packed and possess only a few short neurites (Fig. 3a). In epl_2, terminals of the hemispheres and MB rows 5 and 6 have a diameter of only 1.5–3 μm and the terminals of MB rows 1–4 have a diameter of 3–4 μm (Figs. 4b, 5). The axons of svf3 and svf7 terminate at a slightly deeper level than the axons of svf2 and svf6, with the terminal of svf7 extending the furthest proximally (Fig. 3a).

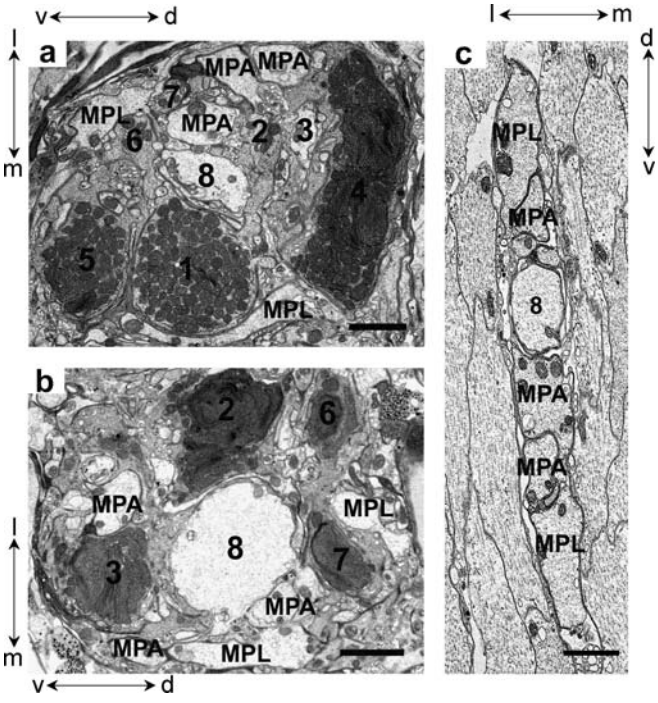

Fig. 4 **a**–**c** Transmission electron micrographs of a lamina cartridge of the dorsal hemisphere of a right eye of *H. glyptocercus* illustrating the arrangement of the short visual fibre (svf) terminals (*1*–*7*) at two lamina strata. The svf terminals are filled with mitochondria and often contain tightly packed membranous tubuli of unknown origin. **a** Frontal section at 5-μm depth into the outer lamina stratum (epl_1). The dilated terminals of svf1, svf4 and svf5 are lined up in the medial half of the cartridge, whereas the axons of svf2, svf3, svf6 and svf7 do not form terminals as yet and are located in the lateral cartridge half. The profiles of the five monopolar ganglion cells (*MPA* and *MPL*) can also be seen. **b** Frontal section at 15-μm depth into the lamina through the inner stratum (epl_2). svf2, svf3, svf6 and svf7 have formed terminals and are rearranged circularly around the enlarged and axially situated long visual fibre (*8*). **c** The axon bundles below the lamina consist of five monopolar ganglion cell axons and the axially situated long visual fibre. The *axes* show the dorsal (*d*) to ventral (*v*) and the medial (*m*) to lateral (*l*) orientations. *Bars* 2 μm

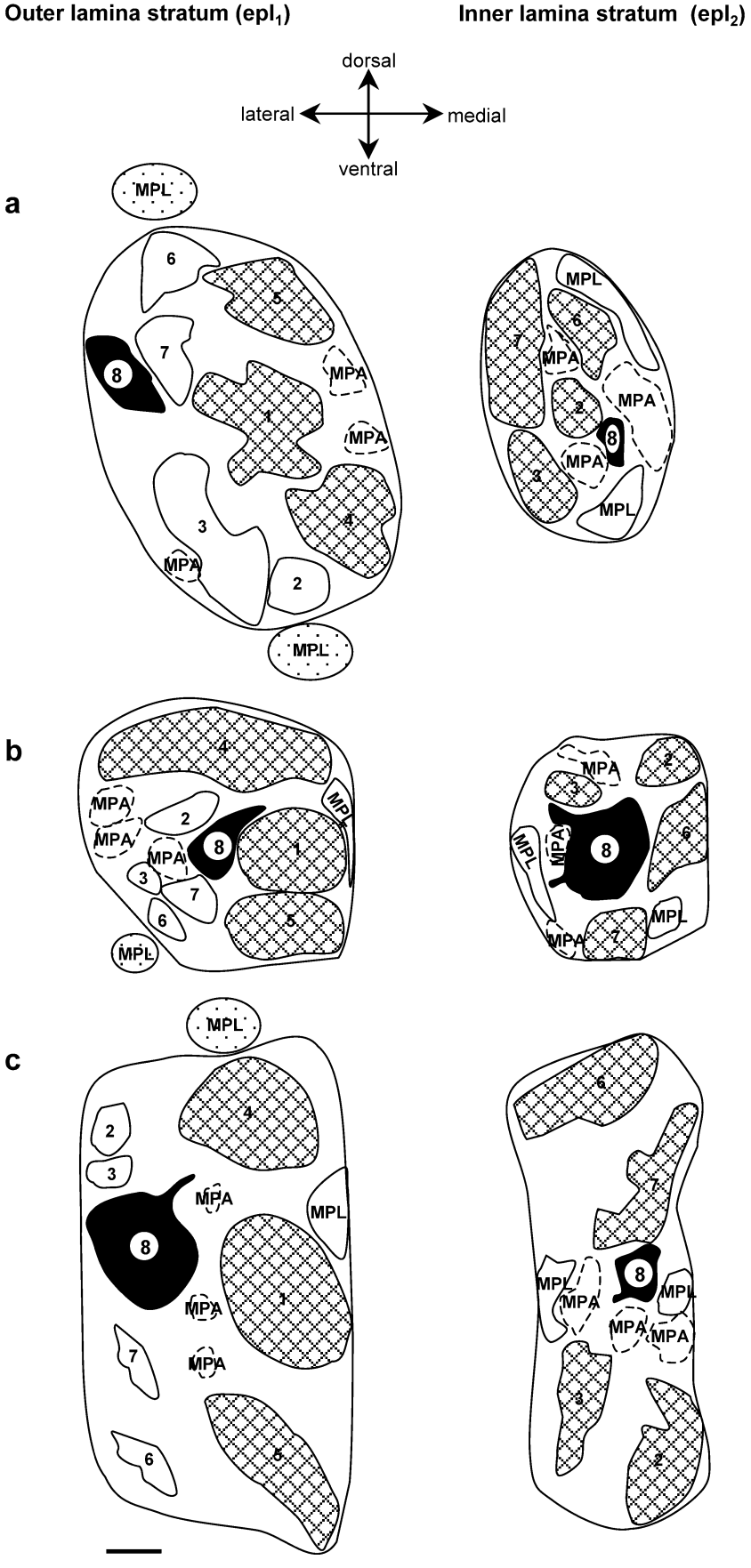

Fig. 5 **a**–**c** Tracings from electron micrographs of frontal sections through a right eye of *H. glyptocercus* showing the regional differences in the photoreceptor axon arrangement at the two lamina strata (epl_1 and epl_2). **a** MB rows 5 and 6. **b** Dorsal hemisphere. **c** MB rows 1 and 2. Because of the mirror symmetry of neuron relationships relative to the equator of the eye, the axon arrangement and numbering within lamina cartridges of the dorsal hemisphere (**b**) and MB rows 1 and 2 (**c**) is mirror-symmetric to the axon arrangement in cartridges of MB rows 3–6 (**a**) and the ventral hemisphere. The profiles of the svfs *1–7* (*white*) and of the long visual fibre *8* (*black*), the terminals of the svfs *1–7* (*chequered*) and the monopolar ganglion cell axons (*white*) and cell bodies (*dotted*) are shown (*MPA* axial monopolar ganglion cell, *MPL* lateral monopolar ganglion cell). *Bar* 2 μm

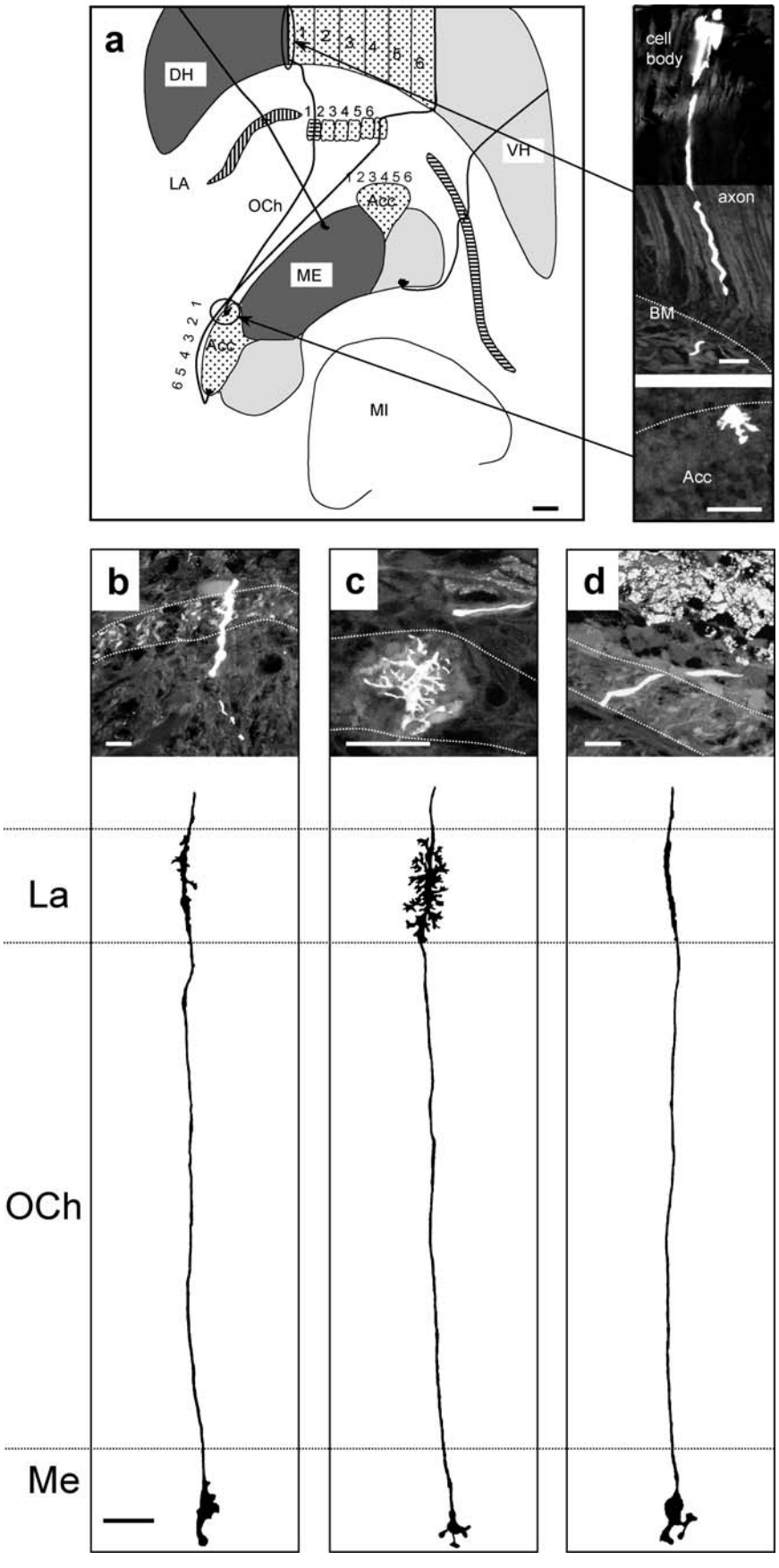

Fig. 6 **a**–**d** The three types of long visual fibres (lvfs). **a** Schematic diagram (*left*) of the retinotopic projection pattern of the lvfs from the three distinct eye regions in a sagittal view of the eye (*1–6* mid-band rows 1–6, *MI* medulla interna, *BM* basement membrane). According to the retinal subsections, the lamina (*LA*) and the medulla externa (*ME*) are also divided into a ventral hemisphere (*VH*) and a dorsal hemisphere (*DH*) part by a mid-band (MB) region (compare with Fig. 1b). The two micrographs (*right*) of 7-μm-thick sagittal plastic sections of a Lucifer-yellow-filled R8 cell of MB row 1 show the cell body in the retina and its terminal in the distal layer of the medulla externa accessory lobe (*Acc*). **b**–**d** *Top* Confocal micrographs of Lucifer-yellow-injected lvfs in 7-μm-thick sagittal plastic sections through the lamina (*dashed outline*). *Bottom* Schematic drawings of the different morphologies of lvfs from the three eye regions. Note that the axons between the *LA* and the *ME*, where they project through the outer optic chiasm (*OCh*), are not shown at their natural lengths. **b** Dorsal and ventral hemispheres. **c** MB rows 1–4. **d** MB rows 5 and 6. *Bars* 25 μm

Different shapes of lamina cartridges

In light-microscopic frontal sections, the shapes of the lamina cartridges of the three eye regions differ (Fig. 2). Hemispheric lamina cartridges (8×10 μm) are smaller than MB lamina cartridges (10×20 μm) and the cartridges of MB rows 5 and 6 are rounded on their dorsal and ventral sides, whereas the cartridges of MB rows 1–4 are rectangular. Electron microscopy has revealed variations in the retinula cell terminal arrangement within the lamina cartridges of the three eye regions, as summarized in Fig. 5.

In frontal sections through the epl_1 of the rectangularly shaped lamina cartridges of MB rows 1–4, the terminals of svf1, svf4 and svf5 are clearly separated from the axons of svf2, svf3, svf6 and svf7 by the axially projecting axons of the lvf and the MPAs. In the lamina cartridges of MB rows 5 and 6, the axons of the MPAs and of the lvf project more peripherally; this allows for a more compact arrangement of the svfs. The svfs of the dorsal (svf5 and svf6) and ventral (svf2 and svf4) sides of the lamina cartridge are shifted medially giving the cartridge an oval shape. Hemispheric lamina cartridges of the epl_1 are hexagonal and, compared with MB lamina cartridges, are compressed in the dorso-ventral direction. The svfs are arranged more compactly around the axially situated lvf and the MPAs occupy a more peripheral position than in MB rows 1–4.

In frontal sections through the lamina cartridges of the epl_2, MB rows 1–4 appear dumbbell-shaped because of the rearrangement of the four remaining receptor terminals of svf2, svf3, svf6 and svf7 in pairs on the dorsal and ventral sides of the cartridge. The axons of the lvf and of the monopolar ganglion cells (MPAs and MPLs) are arranged on the lateral–medial axis of the cartridge. The lamina cartridges of MB rows 5 and 6 appear to be circular in epl_2. The axons of the lvf and of the MPAs are located at the periphery of the cartridge, thereby shifting the photoreceptor terminals closer together. Hemispheric lamina cartridges appear square in the epl_2. The retinula cell terminals, interspersed with the five monopolar ganglion cell axons, are arranged circularly around the lvf. The diameter of the lvf is here notably enlarged (3 μm; Fig. 4b).

Long visual fibres

The lvf originates in the small four-lobed receptor cell situated most distally in the rhabdom (R8; Fig. 6a). Its slender axon (2–3 μm thick) projects from one of the four lobes between the cell bodies of R1 and R7 to the retinal basement membrane, which it penetrates together with the axon of R7 (Fig. 6a). The lvfs project through the lamina, forming characteristic branching patterns for each eye region (Fig. 6b, c). Their trajectories continue across the outer optic chiasm to map retinotopically onto the medulla externa, where they terminate in slightly enlarged endings in the most distal layer of the neuropile (Fig. 6). The terminals expand over an area that covers, in frontal view, the size of a lamina cartridge but is only half as deep (12×12×14 μm). They are club-shaped, sometimes forked or comprising finger-like extensions protruding into the neuropile. No particular terminal shapes can be allocated to certain eye regions.

Three morphologically distinct lvf types can be discerned, based on the presence or absence of spines and the position of their terminals in the medulla externa (Fig. 6b–d). This distinction coincides with the three partitions of the retina: the hemispheres, MB rows 1–4 and MB rows 5 and 6. Hemispheric lvfs terminate in the main body of the medulla externa, the lvfs from the dorsal hemisphere in the dorsal half and the lvfs from the ventral hemisphere in the ventral half (Fig. 6a). MB lvfs terminate in the accessory lobe of the medulla externa (Fig. 6a). The lvfs of MB rows 1–4 form many spiny branching processes within the lamina and extend over the whole cartridge (Fig. 6c). They terminate in four consecutive columns (columns 1–4) within the medulla externa accessory lobe; these columns correspond to the retinal MB rows 1–4 (Fig. 6a). The lvfs of the hemispheres occupy an axial position within the lamina cartridge and their axon diameters increase to about 5 μm in epl_2 (Figs. 4b, 5b). They form lateral neurites, which are less numerous, thicker and shorter than the ones formed by MB rows 1–4 lvfs (Fig. 6b). The lvfs of MB rows 5 and 6 are spineless and terminate in columns 5 and 6 of the medulla externa accessory lobe; these columns correspond to the retinal MB rows 5 and 6 (Fig. 6a, d).

Discussion

We have found that the RCA arrangement in the lamina cartridges of the three eye regions differs. Although the layering of svf terminals into two lamina strata is identical throughout the eye, the arrangement of the svf terminals within each lamina stratum varies. This is presumably dictated by the position of the *en passant* lvf and the MPAs within the lamina cartridges and may be of functional significance. Furthermore, the morphologies of the lvfs of the three eye regions also vary, again suggesting functional differences: those of MB rows 1–4 and of the hemispheres form many spines when projecting through the lamina, whereas the lvfs of MB rows 5 and 6 are spineless.

Svf terminal arrangement in the lamina

Our study demonstrates that the retina-to-lamina projection pattern of the RCAs is identical throughout the eye, regardless of retinal specializations (Kleinlogel et al. 2003). This is also true for the svf terminal arrangement at two distinct lamina strata. The only differences in the ordering of photoreceptor axons within the axon fascicles projecting from the retina to the lamina and of their terminals within the lamina cartridges are attributable to the line of symmetry of the eye between MB rows 2 and 3 (Kunze 1968; Marshall et al. 1991b; Kleinlogel et al. 2003). A striking manifestation of the uniform design in the gonodactyloid lamina is the absence of an effect of the inverted arrangement of the retinula cell groups forming the two rhabdomal

tiers in MB row 2 (Marshall et al. 1991b; Kleinlogel et al. 2003). Although R2, R3, R6 and R7 form the proximal tier in the retina of MB row 2, and not the distal tier as in MB rows 1, 3 and 4, the svfs of these photoreceptors also terminate in the epl_2 as in MB rows 1, 3 and 4.

Another example of common design is found in the polarization-sensitive MB rows 5 and 6. Here, the retinula cell arrangement in the retina of MB row 5 is twisted 90° clockwise in relation to MB row 6, so that each cell group in row 6 possesses microvilli arranged perpendicularly to the microvilli of the same cell group in row 5 (Marshall et al. 1991b). Interestingly, the axon arrangement below the retina and the termination pattern in the lamina are identical for the two polarization rows, i.e. the cell groups of MB row 5 and of MB row 6 terminating in the same lamina stratum are sensitive to orthogonal e-vector directions. The consequence that this may have on polarization processing presents an interesting question for future investigations.

The arrangement of svf terminals at two lamina strata separates the two cell groups possessing either different e-vector or spectral sensitivities. This seems to be an arrangement designed to extract information from two receptor channels within the main rhabdom formed by R1–R7. Where examined in other malacostracan crustaceans, the two lamina strata contain the terminals of the two subpopulations of retinula cells that are sensitive to perpendicular e-vector sensitivities of linearly polarized light (Nässel and Waterman 1977; Stowe et al. 1977; Waterman 1981; Sabra and Glantz 1985). In the crayfish, they have been shown to subserve a polarization opponency system in the medulla externa (Glantz 1996, 2001). We suspect that this is also the case in the MB rows 5 and 6 of the stomatopod, as these are anatomically specialized to mediate polarization vision (Marshall et al. 1991b). However, physiological evidence is lacking. Moreover, we speculate that gonoadactyloid stomatopods adopted the two-stream polarization system of MB rows 5 and 6 to form a two-stream spectral system in MB rows 1–4 for the processing of spectral information. The re-arrangement of the two subpopulations of retinula cells into two retinal tiers in MB rows 1–4 is a modification to allow the serial filtering of light necessary to construct finely tuned spectral sensitivities (Cronin and Marshall 2004). This suggests that serial dichromatic systems may be present in the retinal mid-band rows 1–4. The two subpopulations of svfs terminating at different lamina strata in MB rows 1–4 would then represent spectral opponent pairs, equivalent to the polarization opponent pairs proposed for MB rows 5 and 6 (Marshall et al. 1991b, 1996; Kleinlogel et al. 2003). However, the way in which chromatic information beyond the lamina is processed is unknown. Future morphological and physiological studies of the target neurons of R1–R7, the monopolar ganglion cells, are required to understand the processing of colour and polarization information at the next level.

Although the general svf termination pattern at two lamina strata is identical within the three eye regions, differences exist in the axonal arrangement within each lamina stratum. One reason for differences in the axon packing is the variations in lamina cartridge size, caused by the differently sized overlying corneal facet lenses (Stavenga 1979). The facet lenses of the MB are rectangular in shape, whereas the facet lens mosaic of the hemispheres is of a more compressed hexagonal pattern (Fig. 2). Because the mosaic of the corneal facet lenses is reflected by the neural organization of the retina and the lamina, hemispheric lamina cartridges are also compressed compared with MB lamina cartridges. This leads to a more compact axonal arrangement within the hemispheric lamina cartridges. However, this still does not explain why the packing of svf terminals of MB rows 1–4 differs from the packing of svf terminals of MB rows 5 and 6. We suggest that the differences here are attributable to variations in the location of the *en passant* lvf, which is probably of functional significance for polarization and colour vision.

The findings described are common, so far, for all gonodactyloid species investigated, whereas the deeper-living squilloid stomatopod *Squilla mantis* has previously been reported to have three instead of two retinula cell terminal layers in the lamina (Strausfeld and Nässel 1981; Schiff et al. 1986; Schiff 1987). Other observations are similar to those presented here and the discrepancies are most probably attributable to the irregularity of svf terminal depth in epl_2. The terminal of svf7 extends the furthest proximally and may give the erroneous impression that it terminates in a more proximal lamina stratum than svf2, svf3 and svf6.

Long visual fibres

The lvfs map the retinal mosaic directly upon the medulla externa, where each forms a small terminal in the distal layer of the neuropile. Lvfs are common in insects and crustaceans and their role is generally to transmit UV and polarization information (Strausfeld and Blest 1970; Nässel 1975, 1977; Armett-Kibel and Meinertzhagen 1977; Stowe et al. 1977; Hardie et al. 1981; Strausfeld and Nässel 1981; Zufall et al. 1989). Three morphologically different types of lvfs are found within the three eye regions of gonodactyloids. Hemispheric lvfs possess short lateral processes restricted to certain lamina strata, whereas the lvfs of MB rows 1–4 form many spiny branches extending over the whole lamina cartridge. The lvfs of MB rows 5 and 6 do not possess any spines.

Both spiny and spineless lvfs have been found in other crustaceans. The best-documented example is the violet-sensitive R8 cell of crayfishes. Whereas the lvfs of *Procambarus* possess neurites that lie within the lamina and that have been shown to be devoid of any synaptic contacts (Cummins and Goldsmith 1981; Strausfeld and Nässel 1981), the lamina portions of the lvfs of *Pacifastacus* are spineless, resembling the lvfs of MB rows 5 and 6 of stomatopods. The lvfs of the crabs *Scylla* and *Leptograpsus* and of branchiopod crustaceans bear processes in the lamina but their functions and connectivities have not been investigated as yet (Stowe et al. 1977; Nässel et al. 1978; Strausfeld and Nässel 1981). Lateral processes of lvfs are common in insect laminae and connections to interneurons or svf terminals have been demonstrated in some cases

(Menzel and Blakers 1975; Strausfeld and Nässel 1981; Zeil 1983; Armett-Kibel and Meinertzhagen 1985; Zufall et al. 1989). Functional chemical synapses of lvfs onto monopolar ganglion cells and retinula cells have been described for the ant *Cataglyphis* (Meyer 1979), the bee *Apis* (Ribi 1975, 1981; Souza et al. 1992), the dragonfly *Sympetrum* (Armett-Kibel and Meinertzhagen 1985) and the bibionid fly *Bibio* (Boschek 1971).

The R8 receptors of gonodactyloid stomatopods are sensitive to light in the UV part of the spectrum (Marshall and Oberwinkler 1999). Only in MB rows 5 and 6 do the R8 cells possess unidirectional microvilli, making them likely candidates for polarization sensitivity (Marshall et al. 1991b). Their spineless axons project peripherally through the lamina suggesting that they form an independent neural channel from the R1–R7 cells. Many arthropods use their UV receptors for polarization vision and, therefore, gonodactyloid stomatopods probably use the UV channels of MB rows 5 and 6 as waveband-specific polarization information channels, the signals being neurally processed separate from the polarization opponency channels in the green spectral band formed by the R1–R7 cells (Rossel 1989; Marshall and Oberwinkler 1999; Wehner 2001). One Lucifer-yellow-stained terminal of a MB row 5 lvf possessed lateral connections to the terminal of a neighbouring lvf from MB row 6 within the medulla externa accessory lobe. Such a connection is functionally astute as the R8 cells of MB row 5 and MB row 6 possess orthogonal sets of unidirectional microvilli and could therefore potentially form a UV polarization opponency channel similar to the proposed polarization opponency channel in the green spectral band formed by the R1–R7 cells (Marshall et al. 1991b; Kleinlogel et al. 2003). The nature of this connection has not been investigated in further detail and this is currently our only observation of this lateral interaction.

The R8 receptors of the two hemispheres and of MB rows 1–4 possess orthogonally arranged microvilli (Marshall et al. 1991b); this probably renders them polarization-blind. We speculate that they are spectral receptors. This assumption is supported by the finding that the lvfs of the hemispheres and of MB rows 1–4 possess spines within the lamina; these spines possibly form synaptic contacts with R1–R7 cells. If synaptic connections exist in the lamina, the medulla externa or both neuropiles, R8 might form an opponent pathway with R1–R7 cells. In the hemispheric retina, all R1–R7 cells possess identical spectral sensitivities in the green spectral band (Cronin and Marshall 1989; Marshall et al. 1998). Including the UV sensitivity of the R8 cells, the hemispheres may comprise a two-pigment visual system similar to that suggested for the fiddler crab *Uca* (Hyatt 1975; Horch et al. 2002). At present, MB rows 1–4 of the stomatopod are believed to contain 12 spectral sensitivities sampling the spectrum continuously from 300 to 750 nm (Marshall 1988; Marshall and Oberwinkler 1999; Cronin and Marshall 2004). Eight of these spectral sensitivities reside in the R1–R7 cells (covering the visible part of the spectrum) and four in the R8 cells (covering the UV part of the spectrum). Each MB row 1–4 possesses a pair of spectral sensitivities within the two-tiered main rhabdoms formed by the R1–R7 cells, which are tuned to colourful and behaviourally relevant body markings (Chiao et al. 2000), some of which contain a high UV component (Osorio et al. 1997). If synaptic connections between the R1–R7 cells and the R8 cells exist, each row may contain a trichromatic system formed by the two narrowly tuned spectral sensitivities within the R1–R7 cells and the UV sensitivity of the R8 cell. Alternatively, the R8 cells of neighbouring MB rows (MB rows 1 and 2 and MB rows 3 and 4, respectively), which possess different UV sensitivities (Marshall and Oberwinkler 1999), may form dichromatic channels over the lateral connections of their terminals in the medulla externa. In this case, the colour vision system of the stomatopod would consist of six spectrally opponent channels, two in the UV (neighbouring R8 cells) and four in the visible spectrum (R1–R7 cells of each row). No physiological or behavioural evidence for this exists as yet and investigations into the connectivity of lvfs within the lamina and the medulla externa constitute vital studies for the future.

Conclusions

Our results thus show that each lamina cartridge comprises two layers of svf terminals separating the two retinula cell groups (R1, R4, R5 and R2, R3, R6, R7) with different polarization and spectral sensitivity, respectively. Although the general lamina cartridge structure with two terminal strata is identical throughout the eye, differences in terminal size and arrangement exist between the three eye regions. However, the most striking difference is found in the morphology of the lvf, which originates in the distal R8 cell and forms characteristic branching patterns when projecting through the lamina. Lvfs of MB rows 1–4 and the hemispheres possess spines at the level of the lamina, whereas lvfs of MB rows 5 and 6 are devoid of spines. This suggests that information from the R8 cells of MB rows 1–4 and of the hemispheres is compared with information from the R1–R7 cells at the lamina stage. We speculate that the R8 receptors of MB rows 1–4 are incorporated into the polychromatic system operating at wavelengths beyond 400 nm (formed by R1–R7). In contrast, the R8 receptors of MB rows 5 and 6 appear to form a separate neural channel from R1–R7 for polarization processing. This study provides a basis for future electron-microscopical investigations into the connectivity of photoreceptor terminals (S. Kleinlogel and J. Marshall, unpublished).

Acknowledgements We thank Dr. O. Ganeshina, Dr. N. Hart and Associate Professor S. Collin for constructive comments on the manuscript. We are grateful to R. Webb and R. Gould for their assistance with the electron microscope and to A. Chan for his valuable support with the histology. We also extend our thanks to the helpful staff of the Heron Island Research Station.

References

Armett-Kibel C, Meinertzhagen IA (1977) Cellular and synaptic organisation in the lamina of the dragonfly *Sympetrum rubicundulum*. Proc R Soc Lond [Biol] 196:385–413

Armett-Kibel C, Meinertzhagen IA (1985) The long visual fibers of the dragonfly optic lobe: their cells of origin and lamina connections. J Comp Neurol 242:459–474

Ball E, Kao L, Stone R, Land M (1986) Eye structure and optics in the pelagic shrimp *Acetes sibolgae* (Decapoda, Natantia, Sergestidae) in relation to light–dark adaptation and natural history. Philos Trans R Soc Lond Biol 313:251–270

Bernard GD, Wehner R (1977) Functional similarities between polarization vision and color vision. Vis Res 17:1019–1028

Boschek CB (1971) On the fine structure of the peripheral retina and lamina ganglionaris of the fly, *Musca domestica*. Z Zellforsch 118:369–409

Caldwell RL, Dingle H (1975) Ecology and evolution of agonistic behavior in stomatopods. Naturwissenschaften 62:214–222

Caldwell RL, Dingle H (1976) Stomatopods. Sci Am 234:80–89

Chiao C-C, Cronin TW, Marshall NJ (2000) Eye design and color signaling in a stomatopod crustacean *Gonodactylus smithii*. Brain Behav Evol 56:107–122

Cronin TW, Marshall NJ (1989) Multiple spectral classes of photoreceptors in the retinas of gonodactyloid stomatopod crustaceans. J Comp Physiol [A] 166:261–275

Cronin TW, Marshall NJ (2004) The unique visual world of the mantis shrimp. In: Prete FR (ed) Complex worlds from simpler nervous systems. A Bradford book. MIT, Cambridge, pp 239–268

Cronin TW, Marshall NJ, Quinn CA, King CA (1994a) Ultraviolet photoreception in mantis shrimp. Vis Res 34:1443–1449

Cronin TW, Marshall NJ, Caldwell RL, Shashar N (1994b) Specialisation of retinal function in the compound eyes of mantis shrimps. Vis Res 34:2639–2656

Cummins D, Goldsmith TH (1981) Cellular identification of the violet receptor in the crayfish eye. J Comp Physiol 142:199–202

Glantz MR (1996) Polarization sensitivity in the crayfish lamina monopolar neurons. J Comp Physiol [A] 178:413–425

Glantz MR (2001) Polarization analysis in the crayfish visual system. J Exp Biol 204:2383–2390

Goldsmith TH, Fernandez HR (1968) Comparative studies of crustacean spectral sensitivity. Z Vgl Physiol 60:156–175

Hanström B (1928) Vergleichende Anatomie des Nervensystems der wirbellosen Tiere. Springer, Berlin Heidelberg New York

Hardie RC, Franceschini N, Ribi W, Kirschfeld K (1981) Distribution and properties of sex-specific photoreceptors in the fly *Musca domestica*. J Comp Physiol 145:139–152

Horch K, Salmon M, Forward R (2002) Evidence for a two pigment visual system in the fiddler crab, *Uca thayeri*. J Comp Physiol [A] 188:493–499

Hyatt GW (1975) Physiological and behavioural evidence for colour discrimination by fiddler crabs, Brachyura, Ocypodidae, genus *Uca*. In: Vernberg FJ (ed) Physiological ecology of estuarine organisms. University of Carolina, Columbia, pp 333–365

Kleinlogel S, Marshall NJ, Horwood JM, Land MF (2003) Neuroarchitecture of the color and polarization vision system of the stomatopod *Haptosquilla*. J Comp Neurol 467:326–342

Kunze P (1968) Die Orientierung der Retinulazellen im Auge von *Ocypode*. Z Zellforsch 90:454–462

Land MF, Marshall NJ, Brownless D, Cronin TW (1990) The eye-movements of the mantis shrimp *Odontodactylus scyllarus* (Crustacea: Stomatopoda). J Comp Physiol [A] 167:155–166

Marshall NJ (1988) A unique colour and polarization vision system in mantis shrimps. Nature 333:557–560

Marshall NJ, Land MF (1993a) Some optical features of the eyes of stomatopods. I. Eye shape, optical axis and resolution. J Comp Physiol [A] 173:565–582

Marshall NJ, Land MF (1993b) Some optical features of the eyes of stomatopods. II. Ommatidial design, sensitivity and habitat. J Comp Physiol [A] 173:583–594

Marshall NJ, Oberwinkler J (1999) The colourful world of the mantis shrimp. Nature 401:873–874

Marshall NJ, Land MF, Cronin TW (1989) The structure and function of the mid-band in the eyes of stomatopod crustaceans. J Mar Biol Assoc UK 69:735

Marshall NJ, Land MF, King CA, Cronin TW (1991a) The compound eyes of mantis shrimps (Crustacea, Hoplocarida, Stomatopoda). II. Colour pigments in the eyes of stomatopod crustaceans: polychromatic vision by serial and lateral filtering. Philos Trans R Soc Lond Biol 334:57–84

Marshall NJ, Land MF, King CA, Cronin TW (1991b) The compound eyes of mantis shrimps (Crustacea, Hoplocarida, Stomatopoda). I. Compound eye structure: the detection of polarised light. Philos Trans R Soc Lond Biol 334:33–56

Marshall NJ, Jones JP, Cronin TW (1996) Behavioural evidence for colour vision in stomatopod crustaceans. J Comp Physiol [A] 179:473–481

Marshall NJ, Oberwinkler J, Cronin TW, Land MF (1998) The 16 sensitivities of the stomatopod eye—what are they for? 26th Neurobiology Conference, Göttingen

Menzel R, Blakers M (1975) Colour receptors in the bee eye—morphology and spectral sensitivity. J Comp Physiol 108:11–33

Meyer EP (1979) Golgi–EM-study of first and second order neurons in the visual system of *Cataglyphis bicolor* Fabricius (Hymenoptera, Formicidae). Zoomorphology 92:115–139

Nässel DR (1975) The organization of the lamina ganglionaris of the prawn, *Pandalus borealis* (Kroyer). Cell Tissue Res 163:445–464

Nässel DR (1977) Types and arrangements of neurons in the crayfish optic lamina. Cell Tissue Res 179:45–75

Nässel DR, Waterman TH (1977) Golgi EM evidence for visual information channelling in the crayfish lamina ganglionaris. Brain Res 130:556–563

Nässel DR, Elofsson R, Odselius R (1978) Neuronal connectivity patterns in the compound eyes of *Artemia salina* and *Daphina magna*. Cell Tissue Res 190:435–457

Nilsson DE, Osorio D (1997) Homology and parallelism in arthropod sensory processing. Chapman and Hall, London

Osorio D, Marshall NJ, Cronin TW (1997) Stomatopod photoreceptor spectral tuning as an adaptation for colour constancy in water. Vis Res 37:3299–3309

Reynolds ES (1963) The use of lead citrate at high pH as an electron–opaque stain in electron microscopy. J Cell Biol 17:208–212

Ribi WA (1975) The neurons of the first optic ganglion of the bee (*Apis melifera*). Adv Anat Embryol Cell Biol 50:1–42

Ribi WA (1981) The first optic ganglion of the bee. VI. Synaptic fine structure and connectivity patterns of receptor cell axons and first order interneurons. Cell Tissue Res 215:443–464

Rossel S (1989) Polarization sensitivity in compound eyes. In: Stavenga DG, Hardie RC (eds) Facets of vision. Springer, Berlin Heidelberg New York, pp 298–316

Sabra R, Glantz RM (1985) Polarisation sensitivity of crayfish photoreceptors is correlated with their termination sites in the lamina ganglionaris. J Comp Physiol 156:315–318

Schiff H (1987) Optical and neural pooling in visual processing in crustacea. Comp Biochem Physiol 88A:1–13

Schiff H, Abbott BC, Manning RB (1986) Optics, range-finding and neuroanatomy of the eye of a mantis shrimp, *Squilla mantis* (Linnaeus) (Crustacea; Stomatopoda; Squillidae). Smithsonian Contrib Zool 440:1–32

Souza JD, Hertel H, Ventura DF, Menzel R (1992) Response properties of stained monopolar cells in the honeybee lamina. J Comp Physiol [A] 170:267–274

Stavenga DG (1979) Pseudopupils of compound eyes. In: Autrum H (ed) Handbook of sensory physiology. Springer, Berlin Heidelberg New York, pp 225–313

Stowe S, Ribi WA, Sandeman DC (1977) The organisation of the lamina ganglionaris of the crabs *Scylla serrata* and *Leptograpsus variegatus*. Cell Tissue Res 178:517–532

Strausfeld NJ, Blest AD (1970) Golgi studies on insects. I. The optic lobes of Lepidoptera. Philos Trans R Soc Lond 258:81–134

Strausfeld NJ, Nässel DR (1981) Neuroarchitecture of brain regions that subserve the compound eyes of crustacea and insects. In: Autrum H (ed) Handbook of sensory physiology. Springer, Berlin Heidelberg New York, pp 344–357

Warrant EJ, McIntyre PD (1990) Limitations to resolution in superposition eyes. J Comp Physiol [A] 167:785–803

Waterman TH (1981) Polarisation sensitivity. In: Autrum H (ed) Handbook of sensory physiology. Springer, Berlin Heidelberg New York, pp 283–469

Waterman TH, Fernandez HR (1970) E-vector and wavelength discrimination by retinular cells of the crayfish *Procambarus*. Z Vgl Physiol 68:154–174

Wehner R (2001) Polarization vision—a uniform sensory capacity? Exp Biol 204:2589–2596

Zeil J (1983) Sexual dimorphism in the visual system of flies: the free flight behaviour of male Bibionidae (Diptera). J Comp Physiol 150:395–412

Zufall F, Schmitt M, Menzel R (1989) Spectral and polarized light sensitivity of photoreceptors in the compound eye of the cricket (*Gryllus bimaculatus*). J Comp Physiol [A] 164:597–608